Water Research 106 (2016) 214–222

Contents lists available at ScienceDirect

Water Research

journal homepage: www.elsevier.com/locate/watres

Roles of singlet oxygen and dissolved organic matter in self-sensitized photo-oxidation of antibiotic norfloxacin under sunlight irradiation

Xi-Zhi Niu, Francesco Busetti, Markus Langsa, Jean-Philippe Croué*

Curtin Water Quality Research Centre, Department of Chemistry, Curtin University, GPO Box U1987, Perth, WA 6845, Australia

ARTICLE INFO

Article history:
Received 13 July 2016
Received in revised form
30 September 2016
Accepted 1 October 2016
Available online 4 October 2016

Keywords:
Fluoroquinolone photochemistry
Antibiotic norfloxacin
Singlet oxygen
Dissolved organic matter
Defluorination
Electron transfer

ABSTRACT

Many fluoroquinolone (FLQ) antibiotics undergo rapid photodegradation in sunlit waters and form multifaceted photo-products. The high photodegradation rate is primarily ascribed to their photo-sensitizing properties. Though widely studied, the photo-reaction pathways are not completely revealed; photo-products mediated by different reactive oxygen species are not identified. In our study, photo-degradation of fluoroquinolone norfloxacin was investigated. A rapid degradation in buffered water was observed with a first-order rate constant of 2.45/hr and a quantum yield of 0.039. After light screening correction, selected DOMs (5 mg C/L) slightly enhanced the photodegradation rate with the exception of Suwannee river hydrophobic organic matter (SR-HPO). Three major photo-products were identified using high resolution mass spectrometry (HRMS). With $^1O_2$ dark formation and competitor experiments, norfloxacin self-sensitized $^1O_2$ was found to oxidize norfloxacin by inducing its piperazine chain cleavage. DOMs exhibited a dual role by inhibiting the $^1O_2$-mediated reaction while enhancing the heterolytic defluorination pathway. DOMs were proposed to enhance heterolytic defluorination by donating electron to triplet state FLQ, this proposal was supported with specific UV absorbance (SUVA) as an indicator for the abundance of π bonds. Fluoride formation indicated a 79% elimination ratio of fluorine, an important functional group for antimicrobial activity. This work provides important new insights into the photochemical fate of fluoroquinolone antibiotics in natural water.

1. Introduction

In recent years, antibiotics received increasing attention as prior risk contaminants with omnipresent occurrence and direct ecological risks (Watkinson et al., 2007). Albeit present in environmental waters at very low concentration, antibiotics are able to disrupt important biological processes in waters (Costanzo et al., 2005). They play a significant role in promoting the formation of antibiotic resistance in natural bacteria (Hernando et al., 2006). Fluoroquinolones (FLQs) are among the most commonly prescribed antibiotics for the treatment of many bacterial infections. They are also largely used in aquaculture industry and livestock (Wang et al., 2010). In addition to the general risks inferred to antibiotics, most FLQs exhibit different degrees of photo-toxicity due to their photosensitizing properties (Domagala, 1994; Soldevila et al., 2014). The occurrence of FLQs in surface waters and wastewaters was reported in many countries at different levels. In Switzerland where norfloxacin and ciprofloxacin are the most consumed FLQs, their concentrations in sewage and treated wastewater effluent were in the range of ng/L to μg/L (Golet et al., 2003). Norfloxacin concentration in Hong Kong sewage water was found to reach μg/L level (Leung et al., 2012). Ciprofloxacin content was in the range of 0.2–1.4 μg/L in four wastewater treatment plant (WWTP) effluents from Erie County, New York (Batt et al., 2007). Norfloxacin concentrations in studied WWTP effluents and surface waters from Queensland-Australia reached up to 0.25 μg/L and 1.15 μg/L, respectively (Watkinson et al., 2009). These previous works demonstrate that FLQ antibiotics, in particular norfloxacin and ciprofloxacin, can be detected at relatively high concentration in different effluents and surface waters, a strong motivation to investigate their fate in the aquatic environment. FLQs are not efficiently removed in conventional WWTPs (Watkinson et al., 2007). They are known to sorb onto clay minerals (Nowara et al., 1997), sediments, and sewage sludge (Golet et al., 2002). Kummerer et al (Kümmerer et al., 2000). discovered that, as antimicrobial agents, most FLQs are resistant to microbial degradation. FLQs remain stable to hydrolysis due to the quinolone ring stability

* Corresponding author .
E-mail address: jean-philippe.croue@curtin.edu.au (J.-P. Croué).

http://dx.doi.org/10.1016/j.watres.2016.10.002
0043-1354/

(Babić et al., 2013).

Many FLQs exert significant absorbance in the ultraviolet (UV) and visible light regions (e.g., norfloxacin in Fig. S1), which makes them potential candidate of direct photolysis or photosensitization. As a matter of fact, the complicated photosensitizing properties of irradiated FLQs were widely studied with ultrafast spectroscopic methods (e.g., transient absorbance) (Cuquerella et al., 2004; Lorenzo et al., 2008; Monti et al., 2001; Soldevila et al., 2014), which remains not completely revealed. As ubiquitous antibiotics, FLQs were demonstrated to undergo rapid phototransformation in aquatic systems and various mechanisms were proposed (Ge et al., 2010; Liang et al., 2015; Paul et al., 2010; Porras et al., 2016; Sturini et al., 2012). As photosensitizsers, FLQs are excited upon irradiation and the excited states of FLQs further induce the formation of oxidants such as singlet oxygen ($^1O_2$) (Porras et al., 2016). The presence of naturally occurring sensitizers (e.g., DOMs, pigments, and nitrate) makes the different photochemical pathways of FLQs difficult to distinguish. In the current study, FLQ phototransformation mediated by its triplet states (^{3}FLQ*), and by ^{3}FLQ*-induced reactive oxygen species (ROS) is considered self-sensitized. Ge et al. (2010) found that the self-sensitized hydroxyl radical (·OH) and $^1O_2$ may play important roles in the photodegradation of these antibiotics. The same work also reported that the presence of Fe^{3+} and nitrate reduced the photodegradation rate of FLQs. DOM was found to play an inhibitory effect on the degradation rates of some FLQs (Ge et al., 2010; Liang et al., 2015); the inhibition was more significant when DOMs were used at a high concentration (e.g., 20 mg C/L) (Liang et al., 2015). However, in addition to the effect of DOMs on the photolytic rate of FLQs, their impact on the formation pathways of the FLQ photo-products has not been well described and requires deeper investigation.

Multifaceted photo-products are generated during the photolysis of FLQs. For instance, irradiated ciprofloxacin generated eight different primary photo-products depending on the pH condition (Wei et al., 2013). The major primary photo-products of FLQs were formed via defluorination, piperazine chain cleavage, and photosubstitution (Sturini et al., 2012). According to current mechanistic understanding, defluorination of FLQs is considered to occur from ^{3}FLQ* (Fasani et al., 2001), a reaction that is unlikely to exist in other aromatic fluoride (e.g., fluorobenzenes) due to the high energy level of the C-F bond (Havinga and Cornelisse, 1976). The reaction pathway that does not involve the loss of fluorine while causing *N*-dealkylation on the piperazine side chain is unknown. Although mass spectrometric studies identified many photo-products, the respective pathways elucidating how they are formed are not completely understood. Additionally, the detailed impacts of dissolved organic matter and photo-induced reactive oxygen species (ROS) such as $^1O_2$ are not clear.

In our study, the photochemistry of fluoroquinolone in aqueous solutions under simulated sunlight was investigated with the example of norfloxacin. As aforementioned, photochemically FLQs behave in similar ways and norfloxacin is a representative FLQ antibiotic. Both photo-degradation and photo-products formation kinetics were followed. Among different ROS, the role of $^1O_2$ was revealed using $^1O_2$ dark formation experiment. Fluorine elimination was quantified by following the release of fluoride in solution using ion chromatography. The primary photo-products were identified with high resolution mass spectrometry (HRMS) and tentative reaction pathways with the presence of SR-HPO are proposed. The dual role of DOM in different norfloxacin photodegradation pathways was discussed.

2. Materials and methods

2.1. Reagents and DOM isolates

The chemicals were obtained at the highest purity and used as received: norfloxacin (NOR, 98+%, Fluka analytical), furfuryl alcohol (FFA, 98% Acros Organics), sodium phosphate monobasic/sodium phosphate dibasic (99+%, Ajax Finechem), phosphoric acid (85+% in water, Ajax Finechem), pyridine (PYR, 99+% Fluka Analytical); *p*-nitroanisole (PNA, 98+% Sigma-Aldrich); sodium fluoride (99+% Sigma-Aldrich), L-histidine (99+% Sigma-Aldrich), sodium azide (99+% Sigma-Aldrich), isopropanol (99.8% Acros Organics), sodium bismuthate (80+% Sigma-Aldrich), hydroxyl chloric acid (32% in water, Ajax Finechem), potassium hydroxide (99% Ajax Finechem).

Four purified dissolved organic matter (DOM) isolates (i.e., hydrophobic acid DOM fractions also called fulvic acids) were selected for this study. These include hydrophobic acid fractions from Suwannee River (SR-HPO), Beaufort River (BF-HPO), Seine River (Seine-HPO), and South Platte River (SPR-HPO), previously isolated according to the method reported by Leenheer and colleagues (Leenheer et al., 2000). The stock solutions of DOM and other chemicals were prepared in 5 mM phosphate buffer in ultrapure water (18.2 MΩ cm, Milli-Q, Purelab Classic).

2.2. Photodegradation experiments

The experimental setup for the sunlight simulator (Suntest XLS +, ATLAS, USA) was the same as per described in our previous work (Niu et al., 2014). An energy level of 400 W/m^2 supplied by a xenon arc lamp (NXE 1700, daylight mode) and an internal filter (ATLAS, Cat. 56079197) were used for the simulated irradiation in the wavelength range of 300–800 nm. Additional glass filters (Newport, FSQ-WG320) were placed on top of the reaction solutions, cutting off at 320 nm. The full spectra of the simulated sunlight, both with and without glass filters, were previously measured (Niu et al., 2014). All reactors (10 mL Pyrex reactors) used were painted black to prevent light reflection and were submerged in a circulating water bath set at 25 °C. A refrigerated circulator (Julabo F250) was used to provide thermostat circulating water. All sample solutions were stirred using a multi-point stirrer (Cimarec i Poly 15, Thermo Scientific) set to 200 rpm.

Photodegradation experiments of 5 μM norfloxacin were carried out at a pH of 8.0, buffered by 5 mM phosphate. DOM solutions were used at a TOC of 5 mg C/L. Isopropanol (20 mM) and L-histidine (20 mM) were used as competitors for photosensitized ·OH and $^1O_2$, respectively. Furfuryl alcohol was used as a probe molecule to monitor the production of $^1O_2$. PNA/PYR actinometer (10 μM for PNA and 0.01 M for PYR) was used to determine the photon flux and quantum yield as previously described by Canonica et al. (2008). All experiments were conducted at least in duplicate. Sample aliquots of photo-experiments were analysed immediately after collection.

2.3. Formation of $^1O_2$ under dark condition

$^1O_2$ was formed in dark with sodium bismuthate ($NaBiO_3$) according to protocols proposed by Ding et al (Ding et al., 2015). with some modifications. The reaction solution containing 5 μM of norfloxacin and 2 mg/mL of $NaBiO_3$ was placed in a water bath of 25 °C. After taking the initial sample (T_0), HCl solution was quickly added to the solution, adjusting the solution to a pH of 4.0. The second sample was taken after 10 min (T_1) of contact time. NaN_3 was added to the sample aliquots to scavenge $^1O_2$ residuals. The experimental solution was strictly kept in dark during this process. The samples were then filtered (0.2 μm) for liquid chromatography analysis.

2.4. Analytical procedures

The total organic carbon (TOC) and pH in this study were measured with a TOC analyser (Shimadzu TOC-V) and a pH meter (Thermo Scientific). A spectrophotometer (Cary 60, Agilent) was used to measure the UVa–Vis absorbance of solutions. The fluorescent excitation-emission of norfloxacin was measured with a fluorescence photometer (F-7000, Hitachi). Concentrations of norfloxacin and probe molecules were analysed by High Performance Liquid Chromatography (HPLC) (Agilent 1100) coupled with a Diode Array Detector (DAD). An XDB-C18 column (5 μm, 4.6 × 150 mm, Agilent Technologies) was used for compounds separation. The HPLC-DAD was also used to follow the evolution of emerging peaks of photo-products.

The reaction products were identified with a high resolution mass spectrometry (HRMS) using a Thermo Accela 600 LC system coupled to a LTQ Orbitrap XL mass spectrometer (Thermo Fisher). The electrospray ion source (ESI) was operated in positive ionization mode (+eV). A Kinetex C18 column (100 × 2.1 mm, 3 μm, 100 Å) (Phenomenex, Sydney, Australia) was used for compound separation at a flow rate of 200 μL/min. The mobile phase composition was the same with that of HPLC/DAD analysis. The spray and capillary voltages were set at +3.5 kV and +35 V. Details for HPLC and LC-HRMS settings are available in supporting information (SI) (Table S1&S2).

Fluoride content of irradiated solution was determined using ion-chromatography (ICS-3000 Dionex, Sunnyvale, CA, USA) equipped with an IonPac (R) AS19 ion chromatography column (4 × 250 mm) preinstalled with an IonPac (R) AG19 (4 × 50 mm) (Dionex). The mobile phase was generated using a potassium hydroxide (9 mM) eluent generator at a flow rate of 1.0 mL min^{-1}.

3. Results and discussion

3.1. Photodegradation kinetics

The pH condition was found to have a significant impact on the ionization state and UV–Vis absorbance of FLQs, consequently affecting their photodegradation kinetics and pathways (Ge et al., 2010; Wei et al., 2013). For an analogue to natural waters, our work used a pH of 8.0, where norfloxacin is mainly present in its zwitterionic and anionic forms (Liang et al., 2015). A first-order reaction kinetic model was used to fit the experimental data as described in equation-1 and equation-2.

$$\frac{d[NOR]}{dt} = -\left(\sum k_{ROS}[\mathrm{ROS}][NOR] + k_d[NOR]\right) \quad (1)$$

$$k_{obs} = \sum k_{ROS}[ROS]_{SS} + k_d \quad (2)$$

where k_{ROS} ($M^{-1}s^{-1}$) is the second order rate constant between specific Reactive Oxygen Species (ROS) and NOR, k_d (s^{-1}) is the first order rate constant of NOR photo-degradation that does not involve ROS (e.g., direct photolysis). $[ROS]_{SS}$ represents the steady-state concentration of ROS. Under this kinetic model (equation-2), the reaction was determined as pseudo-first-order with respect to NOR. The observed rate constant (k_{obs} in equation-2) was obtained for all photodegradation experiments with calculated R^2 ranging from 0.99 to 1.0. A pseudo first-order rate constant of 2.45 hr^{-1} was obtained for norfloxacin photodegradation conducted at pH 8.0 in absence of organic matter (Fig. 1-a), corresponding to a photochemical half-life ($T_{1/2}$) of 0.28 h. NOR photodegradation quantum yield (ϕ_{NOR}) was determined in the wavelength range 300–360 nm with equation-3, similar with a wavelength-independent model previously described (Canonica et al., 2008).

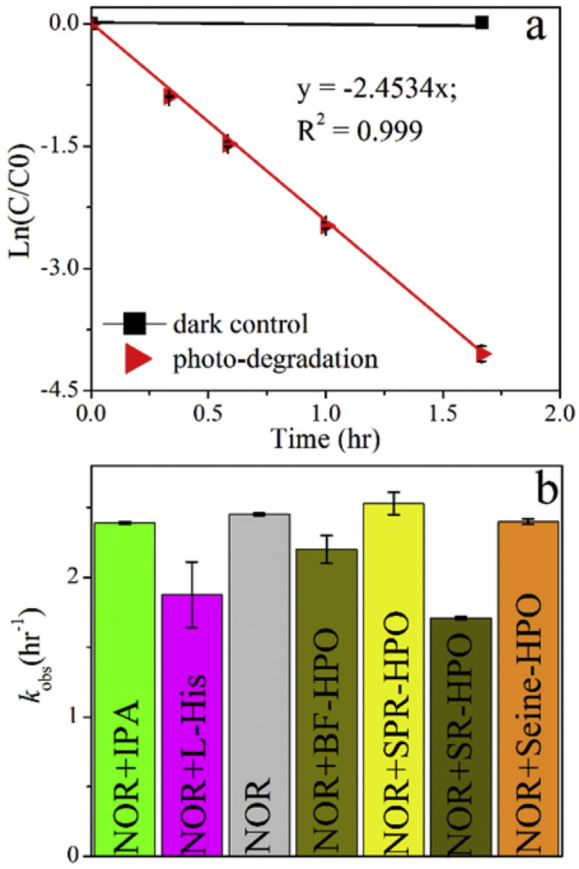

Fig. 1. a) Sunlight-induced degradation of norfloxacin (5 μM) at pH 8.0, 25 °C; b) observed degradation rate constants (k_{obs}) for norfloxacin photodegradation in the presence of ROS competitors (20 mM) (L-His for L-histidine) and different DOMs (5 mg C/L).

$$\phi_{NOR} = \frac{\sum (I_\lambda \cdot \varepsilon_\lambda)_{PNA/PYR}}{\sum (I_\lambda \cdot \varepsilon_\lambda)_{NOR}} \frac{k_{obs\_CR}}{k_{PNA/PYR}} \phi_{PNA/PYR} \quad (3)$$

I_λ is the previously measured irradiance of the sunlight simulator (Niu et al., 2014); ε_λ is the molar absorptivity given in M^{-1} cm^{-1}. k_{obs_CR} is the corrected photodegradation rate of NOR and $k_{PNA/PYR}$ is the corresponding rate constant for PNA degradation, both with a unit of hr^{-1}. $\phi_{PNA/PYR}$ is the quantum yield of the photolysis of the actinometer. Since PYR was used at 0.01 M; this will result in a $\phi_{PNA/PYR}$ of 0.0044 (Leifer, 1988). A ϕ_{NOR} of 0.039 was then obtained in our system. The number here matches well with ϕ_{NOR} values reported in previously studies on photolytic degradation of NOR. For example, one study found a ϕ_{NOR} of ca. 0.043 and 0.013 for zwitterionic and anionic norfloxacin, respectively (Wammer et al., 2013).

The addition of ROS competitors helps to reveal their specific contribution in reaction kinetics and pathways. Isopropanol (IPA) and L-histidine will compete for the ·OH and $^1O_2$ produced in this system (Buxton et al., 1988; Kohn and Nelson, 2007). Our result showed that IPA did not inhibit the photodegradation of NOR (Fig. 1-b); this indicates that ·OH did not make a notable contribution to the overall degradation rate under the current experimental conditions. The $^1O_2$ competitor L-histidine applied an evident inhibitory effect over norfloxacin photodegradation; this result highlighted $^1O_2$ as a significant ROS contributor to the photodegradation process.

As a natural photosensitizer, dissolved organic matter (DOM) is known to enhance the photodegradation rates of many refractory contaminants in waters (Bahnmüller et al., 2014; Canonica et al., 1995). On the other hand, DOM is also sink for ROS, scavenger for reaction intermediates, and a light screener (Canonica and Laubscher, 2008; Wenk and Canonica, 2012; Wenk et al., 2011). Since FLQ photodegradation has been frequently attributed to the self-sensitized ROS and ^{3}FLQ* (Ge et al., 2010; Monti et al., 2001), the presence of DOM could possibly enhance or inhibit (or a balance of the two) the reaction. Fig. 1-b showed the observed norfloxacin photodegradation rate (k_{obs}) in the presence of different DOM fractions. The only DOM isolate for which we did not observe an inhibitory effect over the photodegradation of norfloaxin is SPR-HPO. Although DOMs are photosensitizers, it is likely, from this result, that the $[ROS]_{SS}$ photochemically produced by DOMs was negligible compared to those produced by norfloxacin. As a matter of fact, DOMs were considered to compete for ROS produced by FLQs (Ge et al., 2010). However, light screening effects must be corrected in order to further clarify the role of DOMs in the photoreactions.

In the current system two different photochemical processes were involved in the observed overall reaction: norfloxacin self-sensitization and DOM photosensitization. The light screening correction factor for DOM photosensitized reaction (CF_{DOM}) under sunlight irradiation was calculated in the range of 280–600 nm. The correction wavelength range for norfloxacin self-sensitization was determined at 280–360 nm after measuring its UV–Vis absorbance and fluorescent excitation-emission matrix (FEEM) (Fig. S1&S2). CF_{NOR} (light screening correction factor for norfloxacin self-sensitization) and CF_{DOM} were then calculated separately. The correction and calculation model are available in the SI.

The results suggest that the light screening effect by the studied DOMs (5 mg C/L) should not be overlooked for the self-sensitized degradation of norfloxacin (Table 1). According to the photodegradation rate constants after light screening correction (k_{obs_CR}), BF-HPO did not show observable impact on the photodegradation rate of norfloxacin. SPR-HPO and Seine-HPO only slightly enhanced the phototransformation of norfloxacin. SR-HPO reduced the reaction rate by 11%, corresponding to a negative k_{DOM} (photodegradation rate attributed to this DOM fraction). The potential reason is the scavenging of norfloxacin photochemically produced ROS or reaction intermediates by SR-HPO, while the photosensitizing capacity of SR-HPO is likely much weaker than NOR under the current experimental condition. Compared with SR-HPO, SPR-HPO was found to produce more ^{3}DOM* (based on 2,4,6-trimethylphenol degradation) and $[\cdot OH]_{SS}$ but less $[^1O_2]_{SS}$ (Niu et al., 2014); whereas its aromaticity, a value previously positively correlated to electron donating capacity (EDC) (Aeschbacher et al., 2012), is lower. The slight increase in k_{obs_CR} with the presence of SPR-HPO can be explained with its lower EDC and slightly higher production of ROS than SR-HPO. The overall impacts of DOMs on the photochemical kinetics of norfloxacin degradation vary, depending on the balance of their capacity in ROS production and ROS/reactive intermediates depletion under sunlight.

3.2. Identification of photo-products

The structural and molecular identification of three major photo-products (denoted as P1, P2, and P3) was obtained from LC-HRMS (Table 2) using similar chromatographic separation conditions as those optimized for HPLC-DAD analysis. The tolerance for m/z in positive ESI HRMS was set at 5 ppm. The errors obtained for almost all the compounds and their fragments were lower than 2 ppm. The suggested structures in Table-2 were based on their m/z value and their fragmentation patterns. Similar photo-products were also reported in previous FLQ photochemistry studies (Liang et al., 2015; Paul et al., 2010; Porras et al., 2016; Sturini et al., 2012; Wei et al., 2013). P1 is a result of the piperazine chain photo-cleavage, with the persistence of fluorine on the aromatic ring of quinolone (also found in $^1O_2$ dark formation experiment). P2 also resulted from piperazine chain cleavage, additionally, it underwent heterolysis of the C-F bond. The piperazine chain remained in P3 while the fluorine connected to the quinolone ring was substituted with a –OH group. Although the reconstituted waters in this study may differ from natural waters, these three types of photo-products were also detected in previous investigations where the photochemical fate of FLQs was studied in different surface waters and wastewaters (Babić et al., 2013; Sturini et al. 2012, 2015). Two other molecules that could not be observed on HPLC-DAD chromatograph, i.e., U1 and U2, were detected by HRMS at very low abundance. They are also products of piperazine chain cleavage, likely reaction intermediates of P1 and P2. The LC-HRMS chromatographs and mass spectra are available in SI (Fig. S3).

3.3. Role of singlet oxygen

The formation of $^1O_2$ from irradiated FLQs is a major contributor for their photo-toxicity (Agrawal et al., 2007). Direct visualization of $^1O_2$ with luminescence is very difficult in water (Wilkinson and Brummer, 1981), Martinez and colleagues obtained a $^1O_2$ quantum yield of 0.081 in D_2O (Martinez et al., 1998). Ciprofloxacin (10 mg/L) photochemically generates $^1O_2$ and causes significant *N,N*-dimethyl-*p*-nitrosoaniline (probe molecule) decay under UV-A irradiation in deionized water (Agrawal et al., 2007). Furfuryl alcohol (FFA) is often used in DOM photochemistry as $^1O_2$ probe because it is selective and has a high second order rate constant with $^1O_2$ (1.2×10^8 $M^{-1}s^{-1}$) (Haag and Gassman, 1984). The decay of FFA during the irradiation of norfloxacin was observed and attributed to the production of $^1O_2$ (Fig. S4).

In photochemical experimental conditions, the reaction mechanism of $^1O_2$ is difficult to identify due to the variety of ROS produced and the complexity of FLQ photochemical reactions. In order to further consolidate and clarify the involvement of $^1O_2$ in norfloxacin photochemistry, $^1O_2$ was chemically generated in absence

Table 1
Light screening correction factor (CF), k_{NOM}, k_{obs_CR}, and photochemical half-life of norfloxacin with and without different DOMs.

Samples	CF_{NOR}	CF_{NOM}	k_{NOM}	k_{obs_CR} (hr^{-1})	$T_{1/2}$(hr)[a]	$T_{1/2\_CR}$(hr)[b]
NOR	1.13	–	–	2.77 ± 0.01	0.28	0.25
NOR + BF-HPO	1.24	1.11	negligible	2.77 ± 0.01	0.32	0.25
NOR + SR-HPO	1.32	1.13	−0.3	2.47 ± 0.11	0.41	0.28
NOR + SPR-HPO	1.17	1.08	0.17	2.95 ± 0.2	0.27	0.23
NOR + Seine-HPO	1.22	1.09	0.04	2.81 ± 0.04	0.29	0.25

[a] half-life calculated based on observed rate constant k_{obs}.
[b] half-life calculated based on observed rate constant after correction k_{obs_CR}.

Table 2
Structural and mass spectral data for norfloxacin and its photo-products determined from LC–HRMS.

Compounds	ESI(+), m/z[a]	Structure	Error[b]	Fragments; Molecular mass	Error[b]
Norfloxacin ($C_{16}H_{18}O_3N_3F$)	320.14078	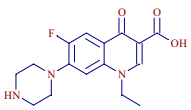	0.887	$C_{16}H_{17}O_2N_3F$; 302.12993 $C_{15}H_{19}ONF$; 276.15067	1.253 0.771
P1 ($C_{14}H_{17}O_3N_3F$)	294.12485		0.023	$C_{16}H_{18}O_3N_3$; 300.13458 $C_{15}H_{20}O_3N_3$; 290.14992	1.040 0.269
P2 ($C_{14}H_{18}O_3N_3$)	276.13437	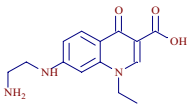	0.370	$C_{14}H_{16}O_2N_3$; 258.12370	0.413
P3 ($C_{16}H_{20}O_4N_3$)	318.14484	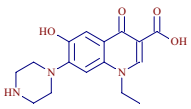	0.829	$C_{14}H_{15}O_2N_3F$; 276.11428 $C_{12}H_{12}O_3N_2F$; 251.08265	0.466 0.211
U1 ($C_{15}H_{18}O_4N_3$)	304.12912	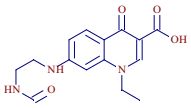	0.206	$C_{15}H_{16}O_3N_3$; 286.11862 $C_{14}H_{18}O_3N_3$; 276.13427 $C_{14}H_{16}O_2N_3$; 258.12370	1.196 0.261 2.196
U2 ($C_{15}H_{17}O_4N_3F$)	322.12073	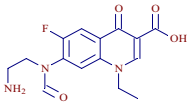	3	$C_{15}H_{14}O_4N_2F$; 305.09322 $C_{14}H_{17}O_3N_3F$; 294.12485	0.552 4.569

[a] m/z values obtained from positive ionization $[M+H]^+$ of molecules during MS analysis.
[b] unit, ppm.

of light and in the presence of norfloxacin. The experimental conditions (i.e., pH and scavengers tested independently in Table S3) used for the production of $^1O_2$ had no impact on norfloxacin. Additionally, a control experiment with the presence of $^1O_2$ competitor was also conducted to confirm the transformation was due to $^1O_2$ (Fig. S5). HPLC-DAD chromatograms of $^1O_2$-norfloxacin reaction products formed under dark condition and norfloxacin photo-products are compared in Fig. 2. The major photo-products as per analysed in Table 2 all had shorter retention time in the C18 column compared with their parent compound (Fig. 2-a) due to an increase in polarity after photo-oxidation. For the dark experiment (Fig. 2-b) the chromatographs recorded for the samples before (red) and after (blue) oxidation were overlapped such that the emerging peak can be easily observed. There was an unknown peak that remained unchanged during the dark reaction (Fig. 2-b), it was found to be impurity from the sodium bismuthate (80+% purity). Only one peak emerged as the product that is ascribed to oxidation by $^1O_2$. By comparing Fig. 2-a and Fig. 2-b, P1 was the compound that could be produced from $^1O_2$ oxidation in photochemical experiment. As a consequence, the formation of P1 was inhibited by $^1O_2$ competitor L-histidine (Fig. 3-a). The two ionisable nitrogen atoms of the piperazine chain from NOR have pK_a values of 8.6 and 10.6 (Qiang and Adams, 2004), respectively. This suggests that the change of the ionization status of the piperazine chain was insignificant when the pH was decreased from 8.0 to 4.0 during the dark experiment. These results qualitatively identified the impact of $^1O_2$ in the photoreaction of norfloxacin by isolating the effect of $^1O_2$ in a dark experiment.

3.4. Reaction mechanisms discussions

3.4.1. $^1O_2$ mediated oxidation

Different DOM fractions showed roughly similar effects on the formation of photo-products under the current experimental conditions (Fig. S6). This could be foreseen considering k_{obs_CR} with DOMs does not significantly differ (Table 1). SR-HPO results were used to illustrate the different roles played by DOM in the formation of P1, P2, and P3 (Fig. 3 a–c). The formation of P1, photo-product originating from $^1O_2$ oxidation, was inhibited by SR-HPO, in accordance with SR-HPO inhibiting the overall photodegradation rate of NOR (Fig. 1-b).

P1 type products were previously identified as photo-product of FLQs, but to our knowledge the reaction mechanism for their formation was not established. Interestingly, P1 type products were produced from the reaction of FLQs with MnO_2 or ClO_2 (Wang et al., 2010; Zhang and Huang, 2005). Likewise, it is not surprising that the piperazine chain cleavage could also be induced by $^1O_2$. A proposed mechanism is given in Fig. 4 (pathway c). $^1O_2$ firstly attacks the piperazine functional group at the N atom (N_1) of the *N*-alkane to give the reaction intermediate c1 (an aniline-like radical cation). N_1, the N atom attached to the aromatic ring of the quinolone structure was found to be more susceptible to oxidation than N_4, the more aliphatic N (Zhang and Huang, 2005). There is evidence that aniline radical cation can be stabilized by the resonance of an adjacent aromatic ring (Laha and Luthy, 1990). This stabilization hereby allows further oxidative reactions on the piperazine side chain rather than a quick deactivation of c1. The aliphatic N_4 is also likely to be oxidized however the reaction rate should be slower. Subsequent oxidation by $^1O_2$ generates iminium

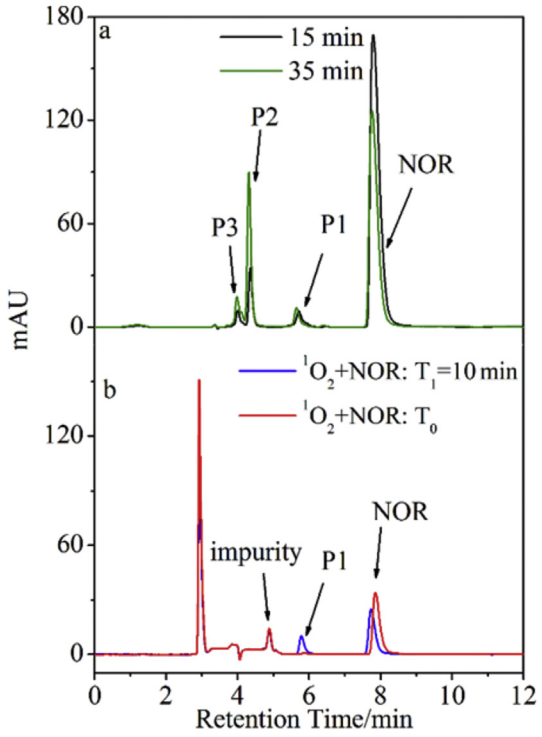

Fig. 2. HPLC-DAD chromatographs of norfloxacin transformation products: a) norfloxacin after 15 min (black) and 35 min (green) of photo-experiment under simulated sunlight; b) norfloxacin before (red) and after 10 min (blue) of dark experiment with bismuthate. (For interpretation of the references to colour in this figure legend, the reader is referred to the web version of this article.)

ions on both N_1 and N_4 (c2). The iminium ions are considered to hydrolyse readily upon formation in aqueous solutions (Smith and March 2007). This combination of oxidation and hydrolysis processes is proposed to lead to the formation of P1. It is possible that SR-HPO inhibits this reaction pathway by scavenging reaction intermediate c1 (reaction c_q in Fig. 4). Similar inhibitory effect was previously reported (Canonica and Laubscher, 2008; Wenk and Canonica, 2012). The photo-induced degradation of aniline and *N,N*-Dimethylaniline was found to be inhibited by 2.5 mg C/L Suwannee River fulvic acid (SRFA), where SRFA was considered to quench the reaction intermediate aniline radical cation (Canonica and Laubscher, 2008). The aniline-like structure of NOR (c1) hereby can also undergo similar quenching process by SR-HPO (i.e., same DOM fraction as SRFA).

3.4.2. *Heterolytic defluorination and photo-substitution*

In FLQ photochemistry, photo-products undergoing both C-F heterolysis and piperazine chain cleavage (e.g., P2) were not found in pure water (Fasani et al., 2001). The formation of P2 type products was thought to be induced by the presence of some inorganic or organic species. As an example, phosphate was considered to mediate an electron-transfer pathway during the defluorination of NOR and enrofloxacin (ENR) upon irradiation (Fasani et al., 2001). In order to avoid potential interferences from phosphate buffer, Wei et al (Wei et al., 2013). used HCl/NaOH to adjust reaction pH in the photochemical experiments of ciprofloxacin (CIP) and products similar to P2 could still be detected. Even phosphate buffer was avoided, halide such as Cl^- can also function as triplet state reductant and form the respective radical anion (Jammoul et al., 2009). As a matter of fact, in real environmental conditions many natural water constituents could lead to electron-transfer to $^3FLQ^*$. Hence, in this work phosphate was still considered an appropriate

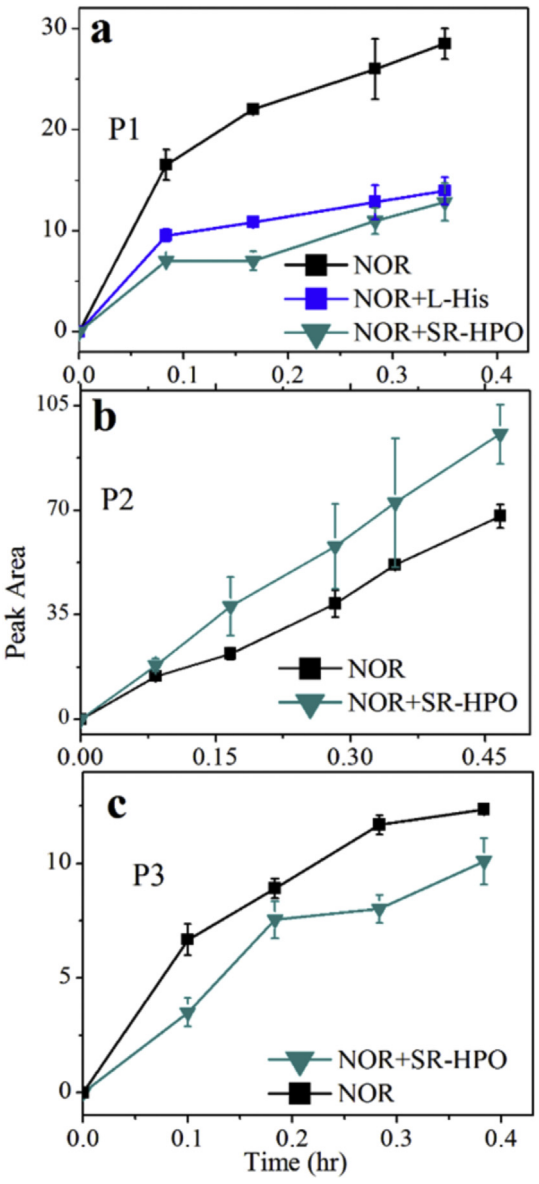

Fig. 3. Evolution of norfloxacin photoproducts.

buffer to investigate the aquatic photochemical processes of FLQ. In the current work, P2, a dominant irradiation product of NOR (Figure-3), was detected and its formation is shown in Fig. 4-b. Unlike the case of P1, the presence of SR-HPO accelerated the formation of P2 (Fig. 3-b).

Upon triplet state NOR ($^3NOR^*$) formation, electron transfer was proposed to occur from an electron donor to $^3NOR^*$. Electron transfer further induces the heterolysis of the C-F bond and the cleavage of the piperazine chain (Albini and Monti, 2003; Fasani et al., 2009). We propose that SR-HPO here is capable of donating electrons to the $^3NOR^*$ (Fig. 4-b) and eventually increasing the formation rate of P2 (Fig. 3-b). Electron donating capacity (EDC) of most organic matter should be significantly higher than buffers (e.g., phosphate in this study). The redox potential (E_h^0) of different humic substances was previously found to be in the range of 0.3–0.6 V vs SHE (standard hydrogen electrode) (Struyk and Sposito, 2001). In particular, the redox potential of IHSS Suwannee River humic acid was found to be 0.778 V at pH 5 and could potentially drop to 0.718 V at pH 8 (Struyk and Sposito, 2001). We

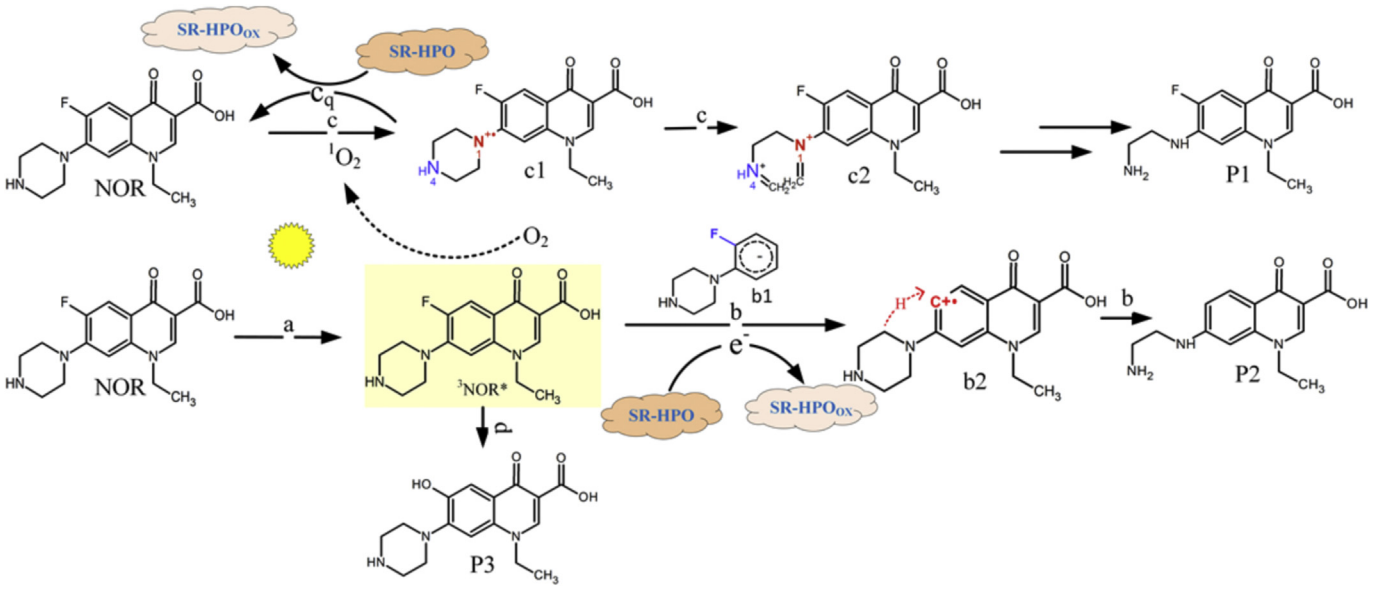

Fig. 4. Proposed mechanism and reaction pathways for self-sensitized photo-transformation of norfloxacin at the presence of SR-HPO; the yellow background of ^{3}NOR* indicates it is in excited state; b1 represents the left side of the quinolone structure (i.e., piperazine side chain connected to fluorobenzene structure) after obtaining electron; SR-HPO$_{OX}$ refers to its oxidized form which could also be a cation radical SR-HPO$\cdot^+$. (For interpretation of the references to colour in this figure legend, the reader is referred to the web version of this article.)

were not able to find the redox potential of ^{3}NOR*/NOR$\cdot$-F (^{3}NOR* reduced by accepting electron), but previous publication referring to CIP (very similar structure with NOR) estimated this value to be higher than 1.45 V (Fasani et al., 2001). With a mediated electrochemical oxidation method (E_h = 0.607 V; mediator: ABTS), Aeschbacher and colleagues reported an EDC of ca. 2.2 mmol-/g for Suwannee River humic acid (SRHA) at pH 8 (Aeschbacher et al., 2012). This indicates that an oxidative potential of 0.607 V induced electron transfer from SRHA at pH 8. Electron donating from SR-HPO is then plausible in our work. A lower redox potential facilitated electron transfer to ^{3}NOR* (b1), while in pure water electron abstraction is difficult to happen. After acquiring electron (b1), the C-F bond split and internal abstraction of H atom from the piperazine chain is considered to happen (b2), leading to the cleavage of the piperazine chain (P2). Similar reaction mechanism involving an intramolecular H atom transfer was also proposed in the photochemistry of some other FLQs (Fasani et al., 2009; Soldevila and Bosca, 2012). To evaluate above proposed mechanism of electron transfer from DOM, P2 formation rate k_{P2_DOM}/k_{P2_ref} determined with the four DOM isolates was plotted against their respective specific UV absorbance at 254 nm or SUVA (Fig. 5-a). The P2 formation rate in the absence of DOM was used as the reference value k_{P2_ref}. There is evidence that π nucleophiles are specifically efficient electron donors in the photo-formation process of these aryl cation (e.g., b2) (Fagnoni and Albini, 2005; Fasani et al., 2009). This makes SUVA a strong surrogate for electron donating group in this reaction, because SUVA correlates well with the relative abundance of unsaturated bonds (incorporating π bonds), e.g., aromatic, alkenes, and alkyne moieties (Croue et al., 1999). Fig. 5-a showed a highly positive correlation between k_{P2_DOM}/k_{P2_ref} and SUVA (R^2 = 0.931). This result supported the afore-discussed hypothesis that DOM functioned as an electron donor, i.e., reductant, and enhanced the formation of P2.

Photosubstitution (d) was considered one of the dominant pathways in pure waters where ^{3}NOR* undergoes substitution of F for OH. The formation of photosubstitution-product P3 was not significantly influenced by the presence of SR-HPO (Fig. 3-c). The slight decrease in P3 formation rate can be compensated after

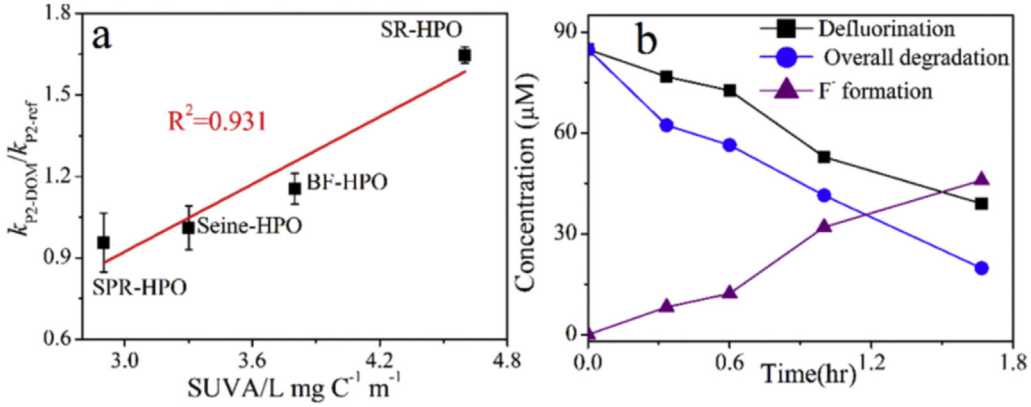

Fig. 5. a) DOM induced increase of P2 formation rate as a function of SUVA; b) fluoride formation, degradation accompanied by defluorination and overall degradation of norfloxacin.

considering a CF of 1.32 for the case of SR-HPO. It is a minor reaction in the current system with DOMs (resulting in electron transfer reaction b) and moderate basicity. P2 & P3 are both results of elimination of fluorine, a functional group considered to give over 10-fold increase in gyrase inhibition for quinolone antibiotics (Domagala, 1994). The photo-induced defluorination was quantified in our work. According to equation-4, NOR underwent defluorination and produced P2 or P3.

$$NOR - F \rightarrow [^3NOR - F^*] \rightarrow P2\&P3 + F^- \quad (4)$$

By following in parallel the release of fluoride ion (F^-) into solution (i.e., 1 mol mole F^- per mole of NOR) and the degradation of NOR, the percentage of NOR losing fluorine can be determined (Fig. 5-b). This result showed that approximately 79% of NOR underwent fluorine elimination under our experimental conditions, indicating that this antibacterial site was predominantly removed. Although photo-induced changes was not followed by the degradation of the quinolone structure (i.e., a basis for FLQ antibacterial potency (Domagala, 1994), the loss of fluorine and the cleavage of the piperazine functional group could be associated with the observed decrease in antibacterial activity. These modifications are considered responsible for reported antibacterial potency changes of photo-degraded FLQs (Paul et al., 2010; Porras et al., 2016).

4. Conclusions

This work provided new insights for the photochemical fate of fluoroquinolone antibiotics. Due to similarity in core structures, the results of this work can also be important reference for the photochemistry of other fluoroquinolone antibiotics such as ciprofloxacin, ofloxacin, levofloxacin, etc. The main findings include:

1). Norfloxacin photodegraded rapidly under simulated sunlight, with a quantum yield of 0.039 (pH = 8.0 in phosphate buffer); after light screening correction, the presence of DOM (5 mg C/L) slightly enhanced the norfloxacin photodegradation rate with the exception of SR-HPO;
2). ROS quenching experiments confirmed the importance of $^1O_2$ for the photo-oxidation of norfloxacin; a $^1O_2$ dark formation experiment helped reveal the corresponding photoproduct to be a result of piperazine chain cleavage;
3). A one-electron-transfer oxidation mechanism was proposed for $^1O_2$-mediated reaction; DOM was found to play an inhibitory role;
4). DOM increased the formation rate of P2 (heterolytic defluorination pathway); the higher the SUVA of DOM the higher the rate of P2 formation, supporting the electron donating role of DOM in this reaction pathway;
5). 79% of the photodegraded norfloxacin underwent defluorination.

Acknowledgment

The authors would like to acknowledge the Australian Research Council (LP130100602), Water Research Australia, Chemcentre and Curtin University for funding this work. Curtin University (Curtin International Postgraduate Research Scholarship) and Water Research Australia (WaterRA PhD Scholarship, 4513-15) are also acknowledged for providing financial support for X.Z. Niu. We thank Zuo Tong How (CWQRC) for assistance in HRMS, Dr. Leonardo Gutierrez (CWQRC) and Dr. Max Massi (Curtin) for useful discussions. We also thank the anonymous reviewers for the helpful comments on the paper.

Appendix A. Supplementary data

Supplementary data related to this article can be found at http://dx.doi.org/10.1016/j.watres.2016.10.002.

References

Aeschbacher, M., Graf, C., Schwarzenbach, R.P., Sander, M., 2012. Antioxidant properties of humic substances. Environ. Sci. Technol. 46 (9), 4916–4925.
Agrawal, N., Ray, R.S., Farooq, M., Pant, A.B., Hans, R.K., 2007. Photosensitizing potential of ciprofloxacin at ambient level of UV radiation. Photochem. Photobiol. 83 (5), 1226–1236.
Albini, A., Monti, S., 2003. Photophysics and photochemistry of fluoroquinolones. Chem. Soc. Rev. 32 (4), 238–250.
Babić, S., Periša, M., Škorić, I., 2013. Photolytic degradation of norfloxacin, enrofloxacin and ciprofloxacin in various aqueous media. Chemosphere 91 (11), 1635–1642.
Bahnmüller, S., von Gunten, U., Canonica, S., 2014. Sunlight-induced transformation of sulfadiazine and sulfamethoxazole in surface waters and wastewater effluents. Water Res. 57, 183–192.
Batt, A.L., Kim, S., Aga, D.S., 2007. Comparison of the occurrence of antibiotics in four full-scale wastewater treatment plants with varying designs and operations. Chemosphere 68 (3), 428–435.
Buxton, G.V., Greenstock, C.L., Helman, W.P., Ross, A.B., 1988. Critical review of rate constants for reactions of hydrated electrons, hydrogen atoms and hydroxyl radicals (• OH/• O− in aqueous solution. J. Phys. Chem. reference data 17 (2), 513–886.
Canonica, S., Jans, U., Stemmler, K., Hoigne, J., 1995. Transformation kinetics of phenols in water: photosensitization by dissolved natural organic material and aromatic ketones. Environ. Sci. Technol. 29 (7), 1822–1831.
Canonica, S., Laubscher, H.-U., 2008. Inhibitory effect of dissolved organic matter on triplet-induced oxidation of aquatic contaminants. Photochem. Photobiological Sci. 7 (5), 547–551.
Canonica, S., Meunier, L., Von Gunten, U., 2008. Phototransformation of selected pharmaceuticals during UV treatment of drinking water. Water Res. 42 (1), 121–128.
Costanzo, S.D., Murby, J., Bates, J., 2005. Ecosystem response to antibiotics entering the aquatic environment. Mar. Pollut. Bull. 51 (1), 218–223.
Croue, J., Debroux, J., Amy, G., Aiken, G., Leenheer, J., 1999. Natural Organic Matter: Structural Characteristics and Reactive Properties. In: Formation and Control of Disinfection By-products in Drinking Water, pp. 65–93.
Cuquerella, M.C, Boscá, F., Miranda, M.A., 2004. Photonucleophilic aromatic substitution of 6-fluoroquinolones in basic media: triplet quenching by hydroxide anion. J. Org. Chem. 69 (21), 7256–7261.
Ding, Y., Xia, X., Ruan, Y., Tang, H., 2015. In situ H+-mediated formation of singlet oxygen from NaBiO 3 for oxidative degradation of bisphenol A without light irradiation: efficiency, kinetics, and mechanism. Chemosphere 141, 80–86.
Domagala, J.M., 1994. Structure-activity and structure-side-effect relationships for the quinolone antibacterials. J. Antimicrob. Chemother. 33 (4), 685–706.
Fagnoni, M., Albini, A., 2005. Arylation reactions: the photo-SN1 path via phenyl cation as an alternative to metal catalysis. Acc. Chem. Res. 38 (9), 713–721.
Fasani, E., Mella, M., Monti, S., Albini, A., 2001. Unexpected photoreactions of some 7-Amino-6-fluoroquinolones in phosphate buffer. Eur. J. Org. Chem. 2001 (2), 391–397.
Fasani, E., Monti, S., Manet, I., Tilocca, F., Pretali, L., Mella, M., Albini, A., 2009. Inter- and intramolecular photochemical reactions of fleroxacin. Org. Lett. 11 (9), 1875–1878.
Ge, L., Chen, J., Wei, X., Zhang, S., Qiao, X., Cai, X., Xie, Q., 2010. Aquatic photochemistry of fluoroquinolone antibiotics: kinetics, pathways, and multivariate effects of main water constituents. Environ. Sci. Technol. 44 (7), 2400–2405.
Golet, E.M., Alder, A.C., Giger, W., 2002. Environmental exposure and risk assessment of fluoroquinolone antibacterial agents in wastewater and river water of the Glatt Valley Watershed, Switzerland. Environ. Sci. Technol. 36 (17), 3645–3651.
Golet, E.M., Xifra, I., Siegrist, H., Alder, A.C., Giger, W., 2003. Environmental exposure assessment of fluoroquinolone antibacterial agents from sewage to soil. Environ. Sci. Technol. 37 (15), 3243–3249.
Haag, W.R., Gassman, E., 1984. Singlet oxygen in surface waters—Part I: furfuryl alcohol as a trapping agent. Chemosphere 13 (5–6), 631–640.
Havinga, E., Cornelisse, J., 1976. Aromatic photosubstitution reactions. Pure Appl. Chem. 47 (1), 1–10.
Hernando, M.D., Mezcua, M., Fernández-Alba, A.R., Barceló, D., 2006. Environmental risk assessment of pharmaceutical residues in wastewater effluents, surface waters and sediments. Talanta 69 (2), 334–342.
Jammoul, A., Dumas, S., D'anna, B., George, C., 2009. Photoinduced oxidation of sea salt halides by aromatic ketones: a source of halogenated radicals. Atmos. Chem. Phys. 9 (13), 4229–4237.
Kohn, T., Nelson, K.L., 2007. Sunlight-mediated inactivation of MS2 coliphage via exogenous singlet oxygen produced by sensitizers in natural waters. Environ. Sci. Technol. 41 (1), 192–197.
Kümmerer, K., Al-Ahmad, A., Mersch-Sundermann, V., 2000. Biodegradability of some antibiotics, elimination of the genotoxicity and affection of wastewater bacteria in a simple test. Chemosphere 40 (7), 701–710.

Laha, S., Luthy, R.G., 1990. Oxidation of aniline and other primary aromatic amines by manganese dioxide. Environ. Sci. Technol. 24 (3), 363–373.
Leenheer, J.A., Croue, J.-P., Benjamin, M., Korshin, G.V., Hwang, C.J., Bruchet, A., Aiken, G.R., 2000. Comprehensive Isolation of Natural Organic Matter from Water for Spectral Characterizations and Reactivity Testing, pp. 68–83.
Leifer, A., 1988. The Kinetics of Environmental Aquatic Photochemistry: Theory and Practice. American Chemical Society.
Leung, H.W., Minh, T., Murphy, M.B., Lam, J.C., So, M.K., Martin, M., Lam, P.K., Richardson, B.J., 2012. Distribution, fate and risk assessment of antibiotics in sewage treatment plants in Hong Kong, South China. Environ. Int. 42, 1–9.
Liang, C., Zhao, H., Deng, M., Quan, X., Chen, S., Wang, H., 2015. Impact of dissolved organic matter on the photolysis of the ionizable antibiotic norfloxacin. J. Environ. Sci. 27, 115–123.
Martinez, L.J., Sik, R.H., Chignell, C.F., 1998. Fluoroquinolone antimicrobials: singlet oxygen, superoxide and phototoxicity. Photochem. Photobiol. 67 (4), 399–403.
Monti, S., Sortino, S., Fasani, E., Albini, A., 2001. Multifaceted photoreactivity of 6-Fluoro-7-aminoquinolones from the lowest excited states in aqueous media: a study by nanosecond and picosecond spectroscopic techniques. Chem. A Eur. J. 7 (10), 2185–2196.
Niu, X.-Z., Liu, C., Gutierrez, L., Croué, J.-P., 2014. Photobleaching-induced changes in photosensitizing properties of dissolved organic matter. Water Res. 66, 140–148.
Nowara, A., Burhenne, J., Spiteller, M., 1997. Binding of fluoroquinolone carboxylic acid derivatives to clay minerals. J. Agric. food Chem. 45 (4), 1459–1463.
Paul, T., Dodd, M.C., Strathmann, T.J., 2010. Photolytic and photocatalytic decomposition of aqueous ciprofloxacin: transformation products and residual antibacterial activity. Water Res. 44 (10), 3121–3132.
Porras, J., Bedoya, C., Silva-Agredo, J., Santamaría, A., Fernández, J.J., Torres-Palma, R.A., 2016. Role of humic substances in the degradation pathways and residual antibacterial activity during the photodecomposition of the antibiotic ciprofloxacin in water. Water Res. 94, 1–9.
Qiang, Z., Adams, C., 2004. Potentiometric determination of acid dissociation constants (pK a) for human and veterinary antibiotics. Water Res. 38 (12), 2874–2890.
Smith, M.B., March, J., 2007. March's Advanced Organic Chemistry: Reactions, Mechanisms, and Structure. John Wiley & Sons.
Soldevila, S., Bosca, F., 2012. Photoreactivity of fluoroquinolones: nature of aryl cations generated in water. Org. Lett. 14 (15), 3940–3943.
Soldevila, S., Cuquerella, M.C., Bosca, F., 2014. Understanding of the photoallergic properties of fluoroquinolones: photoreactivity of lomefloxacin with amino acids and albumin. Chem. Res. Toxicol. 27 (4), 514–523.
Struyk, Z., Sposito, G., 2001. Redox properties of standard humic acids. Geoderma 102 (3), 329–346.
Sturini, M., Speltini, A., Maraschi, F., Pretali, L., Ferri, E.N., Profumo, A., 2015. Sunlight-induced degradation of fluoroquinolones in wastewater effluent: photoproducts identification and toxicity. Chemosphere 134, 313–318.
Sturini, M., Speltini, A., Maraschi, F., Pretali, L., Profumo, A., Fasani, E., Albini, A., Migliavacca, R., Nucleo, E., 2012. Photodegradation of fluoroquinolones in surface water and antimicrobial activity of the photoproducts. Water Res. 46 (17), 5575–5582.
Wammer, K.H., Korte, A.R., Lundeen, R.A., Sundberg, J.E., McNeill, K., Arnold, W.A., 2013. Direct photochemistry of three fluoroquinolone antibacterials: norfloxacin, ofloxacin, and enrofloxacin. Water Res. 47 (1), 439–448.
Wang, P., He, Y.-L., Huang, C.-H., 2010. Oxidation of fluoroquinolone antibiotics and structurally related amines by chlorine dioxide: reaction kinetics, product and pathway evaluation. Water Res. 44 (20), 5989–5998.
Watkinson, A., Murby, E., Costanzo, S., 2007. Removal of antibiotics in conventional and advanced wastewater treatment: implications for environmental discharge and wastewater recycling. Water Res. 41 (18), 4164–4176.
Watkinson, A., Murby, E., Kolpin, D., Costanzo, S., 2009. The occurrence of antibiotics in an urban watershed: from wastewater to drinking water. Sci. Total Environ. 407 (8), 2711–2723.
Wei, X., Chen, J., Xie, Q., Zhang, S., Ge, L., Qiao, X., 2013. Distinct photolytic mechanisms and products for different dissociation species of ciprofloxacin. Environ. Sci. Technol. 47 (9), 4284–4290.
Wenk, J., Canonica, S., 2012. Phenolic antioxidants inhibit the triplet-induced transformation of anilines and sulfonamide antibiotics in aqueous solution. Environ. Sci. Technol. 46 (10), 5455–5462.
Wenk, J., Von Gunten, U., Canonica, S., 2011. Effect of dissolved organic matter on the transformation of contaminants induced by excited triplet states and the hydroxyl radical. Environ. Sci. Technol. 45 (4), 1334–1340.
Wilkinson, F., Brummer, J.G., 1981. Rate constants for the decay and reactions of the lowest electronically excited singlet state of molecular oxygen in solution. J. Phys. Chem. Ref. Data 10 (4), 809–999.
Zhang, H., Huang, C.-H., 2005. Oxidative transformation of fluoroquinolone antibacterial agents and structurally related amines by manganese oxide. Environ. Sci. Technol. 39 (12), 4474–4483.